

# Inside Qubic’s Selfish Mining Campaign on Monero: Evidence, Tactics, and Limits

Suhyeon Lee<sup>\*†</sup> and Hyeongyeong Kim<sup>‡</sup>

<sup>\*</sup>Tokamak Network <sup>†</sup>Hashed Open Research <sup>‡</sup>Korea University

**Abstract**—We analyze Qubic’s publicly claimed selfish mining attack against Monero in 2025. By combining measurements from Monero nodes, the Qubic pool API, and Qubic-network observations, we reconstruct Qubic-attributed blocks and effective hashrate and identify ten intervals consistent with block withholding and strategic release. During these intervals, Qubic’s average hashrate share rises to 23–34%, yet we never observe sustained majority control. We evaluate the attack using the classical selfish mining model and a Markov-chain variant that captures Qubic’s conservative release policy. At the inferred parameters, both models predict revenues below honest mining, and our measurements largely confirm this while showing systematic deviations. We attribute the gap to hashrate variability, coarse-grained interval detection, and operational frictions under community countermeasures. We further argue that selfish mining should be analyzed under time-varying hashrate. Even when the average hashrate stays below the static break-even point, an attacker can still run a profitable selfish-mining operation by operating it intermittently.

**Index Terms**—Blockchain, Proof-of-Work, Selfish Mining, Monero

## I. INTRODUCTION

Selfish mining is a form of strategic deviation in proof-of-work systems where a miner withholds blocks and releases them selectively, potentially increasing its share of rewards while weakening confirmation reliability [1]. While the mechanics are conceptually simple, establishing what happened in a real deployment is difficult: the most important actions are precisely the ones that are not broadcast immediately.

In August 2025, the Monero network faced a high-profile episode in which the Qubic mining pool rapidly increased its presence and publicly described its activity as a “51% takeover” and a demonstration of selfish mining [2], [3]. This incident triggered an immediate practical question beyond public dashboards: what actually occurred on chain, how the campaign was executed operationally, and whether it was economically effective or primarily disruptive.

Answering these questions is especially challenging in Monero. Blocks do not carry explicit pool identifiers, and key signals of selfish mining are off-chain by design. We therefore reconstruct the campaign by combining

multiple vantage points. We collect main-chain and orphan blocks from Monero nodes, use Qubic pool job notifications to track its mining view, and incorporate external artifacts shared by the Monero community to strengthen attribution and timing. With these measurements, we infer intervals consistent with withholding and strategic release, quantify orphaning and reorganization effects, and evaluate profitability under both the classical selfish mining model and a campaign-informed variant that captures Qubic’s conservative release behavior. We make the following contributions:

- **Data collection and release.** We collect and release a multi-source dataset that combines node-observed main-chain and orphan blocks with pool-side signals and external artifacts, enabling reproducible analysis of the Qubic incident.
- **Strategy analysis and modeling.** We analyze the observed campaign behavior and formalize a campaign-informed selfish-mining variant to evaluate profitability against standard baselines.
- **Intermittent selfish mining under dynamics.** Based on the observed operation, we highlight that intermittent strategy switching can make selfish mining revenue-improving even below the classical hashrate threshold under standard difficulty adjustment.

**Organization.** Section II reviews related work. Section III describes our data sources and reconstruction methodology. Section IV characterizes Qubic’s mining presence and its effects on orphaning and reorganizations. Section V analyzes Qubic’s selfish mining behavior and evaluates profitability under classical and modified models. Section VI investigates the discrepancy between theoretical expectations and observed revenue. Section VII introduces our time-varying hashrate and intermittent switching abstraction. Section VIII discusses operational dynamics observed during the campaign. Section IX covers mitigation discussions and limitations. Section X concludes.

## II. RELATED WORK

**Selfish mining and strategy variants.** Selfish mining was formalized as a profitable deviation under specific

network and propagation assumptions [1]. Follow-on work generalized the attacker’s strategy space, including eclipse variants [4]. Other work studied optimal and efficiently computable selfish-mining policies using Markov decision processes [5], [6], and examined how profitability and thresholds change across protocols such as Ethereum [7]. Our work builds on these foundations but focuses on what can be validated in a real campaign where internal attacker state is not observable and attribution is difficult. Recent work has also provided statistical/empirical tools for detecting selfish-mining-like behavior in real PoW systems [8].

**Propagation, forks, and difficulty dynamics.** Propagation delays and network asymmetries shape stale blocks and tie-breaking, and are central to selfish mining performance [9], [10]. Beyond generic propagation effects, Monero’s network-layer attack surface has been studied in the context of eclipse-style isolation [11]. Prior work further showed that difficulty adjustment can interact with variable hash power and adversarial strategies to create unstable throughput or cyclic effects [12].

**Defenses and mitigations.** A diverse set of defense approaches have been proposed, including Fresh Bitcoins [13], Zeroblock [14], and Publish-or-Perish style mechanisms [15]. Alternative designs such as Fruitchains [16] and StrongChain [17] explore fairness and transparency in PoW consensus. In parallel, operational discussions in the Monero community have proposed pool-level detective mining and Publish-or-Perish-inspired mitigations [18], [19]. Finally, analyses of mining-pool data publication highlight observability/attribution side channels that can matter for incident validation [20].

### III. DATA COLLECTION

In this section, we present the data collection and processing methodologies for analysis. See Appendix A for dataset and analysis code.

#### A. Block and mining information collection

For analysis, we combine three data sources: Monero block information by Monero nodes, mining job information extracted from Qubic pool job-notification traffic, and Qubic-related block data obtained by monero community via packet sniffing of Qubic network traffic.

**Monero block information.** We needed to operate a Monero pruning node, which is a lightweight Monero node that stores only recent blocks while still participating fully in network validation. Pruning nodes help us not only to collect block data trustfully but also to collect Monero orphan blocks that are not accessible from open Monero explorers. We operated the node from September 29, 2025 — October 17, 2025, which allowed us to reliably collect main-chain blocks as well

as locally observable orphan blocks. For earlier periods, we complemented historical block and coinbase data by querying publicly accessible Monero full nodes via RPC; to improve orphan coverage, we probed 20 public nodes, selected the five most responsive ones, and periodically synchronized their orphan observations. Nevertheless, public node based collection does not guarantee complete coverage of all orphan blocks, and pool-specific orphan blocks may remain partially unobserved.

**Qubic mining pool.** We used the RPC API of the Qubic mining pool to retrieve mining jobs at 5-second intervals. The API has a structure similar to the Stratum protocol, which is widely used by PoW mining pools, and is openly accessible. Specifically, the `job_notify` method returns multiple values, including the mining block height and the previous block hash, enabling miners to obtain the most recent mining jobs. These data are therefore useful for analyzing how Qubic performs selfish mining on the Monero network.

**3rd-party Qubic block dataset.** Finally, we obtained an additional dataset of Qubic-related blocks from the Monero community (See Acknowledgement for attribution), collected via packet sniffing of Qubic network traffic. We merge this third-party dataset with our local/public Monero node observations to supplement Qubic blocks that may be missed by on-chain observation, especially orphan blocks. Notably, the provided dataset contains 22 blocks that were never observed by public infrastructure or our node, suggesting limited propagation.

#### B. Qubic block attribution

Since Monero provides a strong privacy at default, miners cannot be directly identified solely from the blockchain. Block rewards are paid through a special *coinbase transaction*, and while some mining pools optionally disclose a view key to prove ownership of the reward output, this practice is not mandatory. Qubic likewise does not provide view keys in real time, so it is not possible to immediately determine whether a given block was produced by Qubic through straightforward verification only with on-chain data.

Empirically, Qubic’s mining activity appears to be organized into weekly epochs. In general, an epoch ends on Wednesday, and the view key used during that period is disclosed only after the epoch has fully completed, via Qubic’s official Discord channel. A consolidated list of the publicly disclosed Qubic view keys used in our study is given in Table II in Appendix A. Because view keys are disclosed only after an epoch ends, we cannot perform immediate verification with the corresponding view key during an ongoing epoch. However, view-key-based verification itself can be applied regardless of whether a block is included in the main chain, as

TABLE I: Examples of `extra_nonce` values in coinbase transactions from Qubic and non-Qubic pools.

Blocks by Qubic pool	Blocks by Other pools
<code>extra_nonce</code>	<code>extra_nonce</code>
a18300008f031173362951280000000000	3d5bf9d77da9ba00000000000000000000
8e8300008f0311735d0637400000000000	000000000000001337bcdecc400
718300008f031173a0010000000000000000	00000003cd754c000000000000000000000
638300008f0311733f020000000000000000	f8b08baa
5a8300008f0311734f0c0b28000000000000	0000000000000001829d427bb00
ed8200008f031173c2271b30000000000000	00000000000000065c66da4e1000000100000cb7000000000000000000000000000000

long as the raw block data are available, in particular the coinbase transaction and its `tx_extra`. The same procedure can therefore be applied to orphan blocks as well. In our study, the constraint in data collection was not an inherent limitation of the verification method, but a data accessibility issue: for periods prior to running our node, we could not fully collect the raw data of orphan blocks, which limited the scope of application.

To address this limitation, we leverage the `tx_extra` field of coinbase transactions as an additional attribution signal. This field contains an `extra_nonce` area where mining pools may freely embed auxiliary data. By examining blocks suspected to be mined by Qubic, we observe a consistent structural pattern in the `extra_nonce` values. This pattern is highly atypical in ordinary Monero transactions and exhibits a distinctive form that enables us to classify Qubic blocks even before the corresponding view key is published. Furthermore, for all blocks that were later confirmed to belong to Qubic through `ex-post` view key disclosure during our study period, we did not observe any violations of this pattern.

Table I presents representative examples of `extra_nonce` values observed in Qubic blocks and in blocks from other mining pools. Based on these samples, we could identify three heuristic regex patterns that capture the Qubic-specific structure of the `extra_nonce`. The patterns are provided in Appendix A.

We classify a block as mined by Qubic if the `extra_nonce` of its coinbase transaction matches this pattern. This method enables us to attribute Qubic-mined blocks across the Monero blockchain without requiring any private keys or pool-disclosed view keys.

#### IV. QUBIC’S MINING ON MONERO

This section characterizes Qubic’s presence on the Monero network during the observation period. We first quantify its mining power based on attributed blocks, and then examine its impact on orphan blocks and reorganizations. A focused analysis of Qubic’s selfish mining strategy follows in Section V.

##### A. Qubic’s mining power share

Figure 1 shows Qubic’s mining power share in the Monero network, computed as the ratio of Qubic-attributed blocks to all main-chain and orphan blocks

over weekly, daily, and hour windows. Since direct telemetry of the pool’s physical hashrate is unavailable, we rely on this ‘effective hashrate’ realized on-chain as the primary metric ( $\alpha$ ) for our selfish mining models. It was measured by the number of blocks share over the total blocks in a period. This approach prioritizes realized block production over nominal hardware performance (hash/s), as the former directly determines the success probability of chain reorganizations. Throughout the measurement period, Qubic’s overall average share is approximately 22.09%, far below a sustained majority of the network hashrate.

A central point in public discussions was Qubic’s claim, echoed by several media outlets, that it had achieved a 51% mining position on Monero. However, the notion of a “51% attack” is often left ambiguous, and our measurements do not support a persistent majority. In the 6-hour series, we observe several short intervals where Qubic’s share approaches or briefly exceeds 50% [2]. In contrast, the corresponding daily and weekly aggregates never reach 51%, and Qubic does not maintain a stable majority at any point in our dataset. These results indicate that while Qubic temporarily concentrated substantial mining power, it did not achieve the sustained control typically associated with a practical 51% attack on the Monero network.

##### B. Orphan Blocks by Qubic

Although Qubic did not sustain majority mining power, its activity significantly affected the stability of the Monero chain when it engaged in selfish mining. Selfish mining naturally leads to frequent chain reorganizations, which manifest as orphan blocks on the public chain.

Figure 2 presents the daily counts of regular and orphan blocks, separated into Qubic-attributed and non-Qubic blocks, alongside the average network difficulty. We observe a pronounced increase in the number of orphan blocks during periods when Qubic is active with selfish mining, including a substantial fraction attributable to Qubic itself. This behavior indicates that Qubic’s strategy not only discarded other miners’ blocks but also caused a non-trivial number of its own blocks to be orphaned.

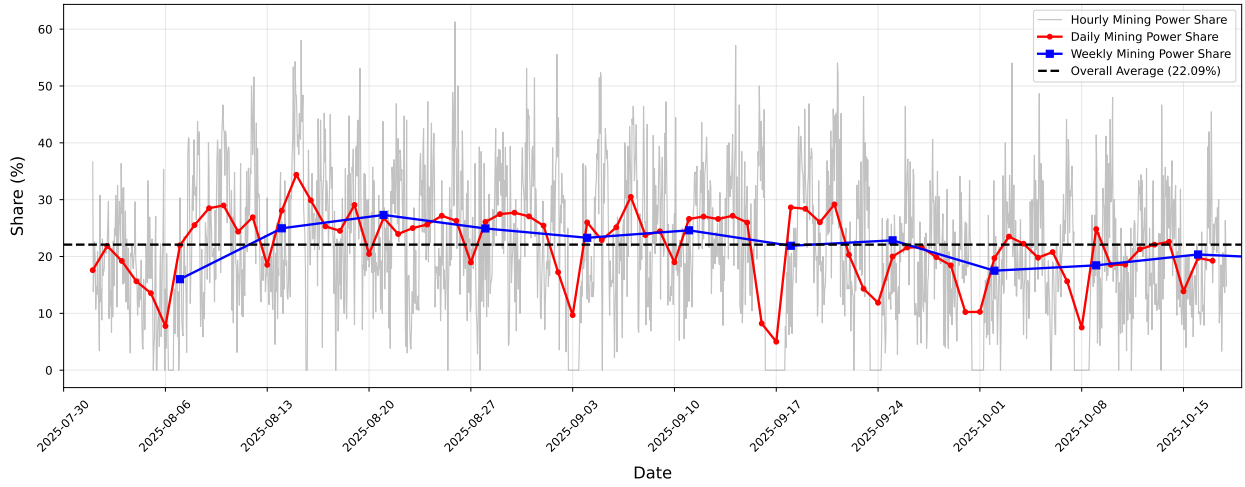


Fig. 1: Qubic mining pool's mining power share on the Monero network

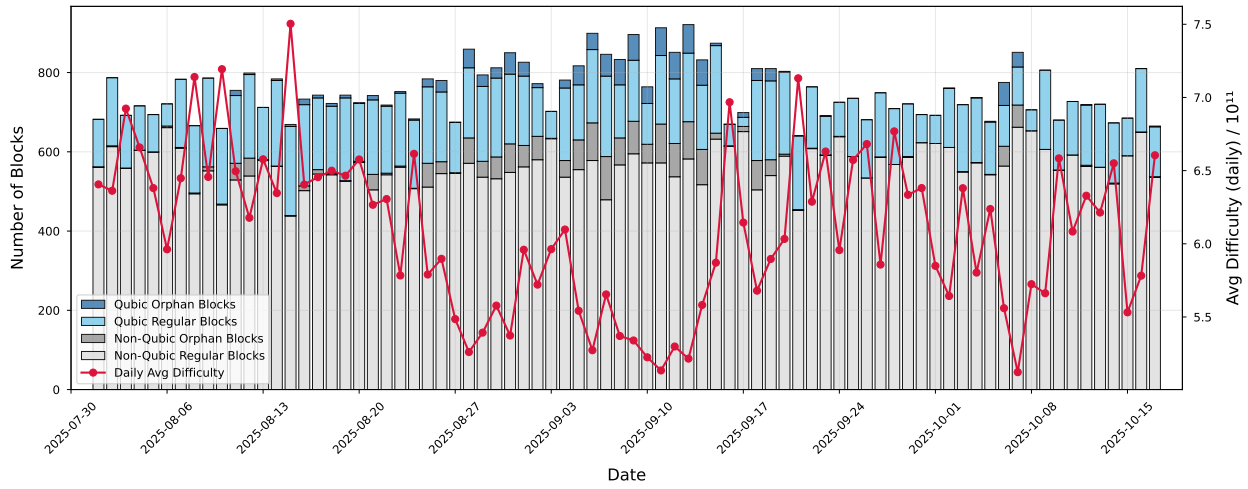


Fig. 2: Daily Monero chain block production

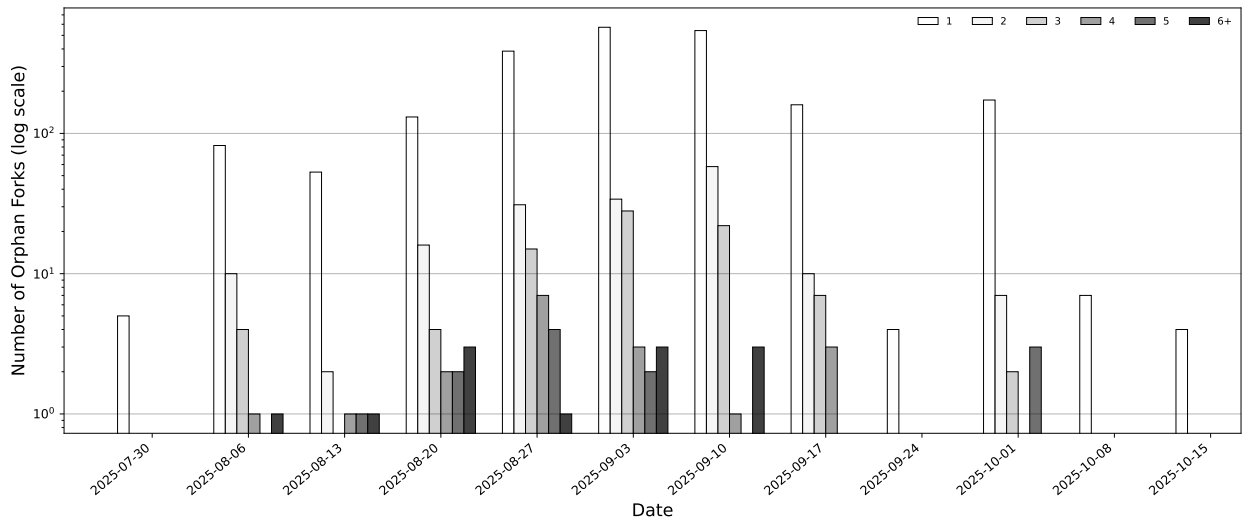


Fig. 3: Weekly distribution of orphan lengths

Figure 3 shows the distribution of orphan fork lengths over time. In periods without Qubic’s selfish mining, orphan forks are almost exclusively of length one. Once Qubic’s selfish mining begins, we observe a clear shift toward longer orphan chains, with more frequent occurrences of multi-block forks. This change reflects deeper and more disruptive reorganizations of the main chain.

## V. SELFISH MINING FOCUSED ANALYSIS

In this section, we analyze Qubic’s selfish mining behavior on Monero and evaluate the profitability of the inferred strategy. We first outline the strategic context, then justify our use of Qubic’s timestamps, identify candidate selfish mining periods, formalize the corresponding analytical model, and finally compare the theoretical revenue with Qubic’s observed mining share.

### A. Selfish mining strategies

Classical selfish mining strategies, as introduced by Eyal and Sirer [1] and later optimized by Sapirshtein et al. [5], describe how a rational miner (or pool) withholds blocks and selectively publishes a private chain to gain a revenue share exceeding its relative hashrate. In practice, miners face uncertainty due to network asynchrony and incomplete information, and may adapt their withholding and release rules accordingly. Qubic’s publicly visible behavior and self-reported capabilities suggest the possibility of such deviations, but its exact internal policy remains unobservable.

Our analysis is therefore necessarily indirect. We do not assume access to Qubic’s internal block discovery times or private chain states. Instead, we rely on Monero main-chain and orphan blocks, Qubic-attributed blocks, and their timestamps to infer when and how Qubic may have executed selfish mining. The following subsections validate our use of timestamps for this purpose and identify periods in which Qubic’s behavior is consistent with sustained strategic deviation, which we subsequently interpret through an analytical model.

### B. Reliability of Qubic block timestamps

To infer Qubic’s strategy from on-chain artifacts, we must first assess whether Qubic’s block timestamps are usable as approximate indicators of block discovery and release behavior. We focus on heights where a Qubic block competes with at least one orphan block or where Qubic’s block itself becomes orphaned, and measure the timestamp differences between Qubic-attributed blocks and competing blocks.

As illustrated in Fig. 4, in the majority of competing blocks, Qubic’s blocks exhibit timestamps that are either antecedent to or comparable with those of competing blocks. This temporal alignment is consistent

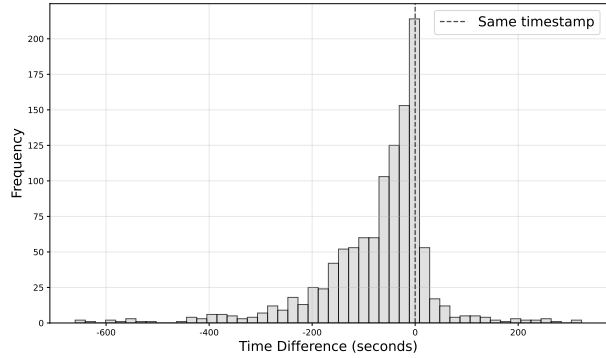


Fig. 4: Qubic blocks’ timestamp difference distribution with the same height blocks including orphan blocks

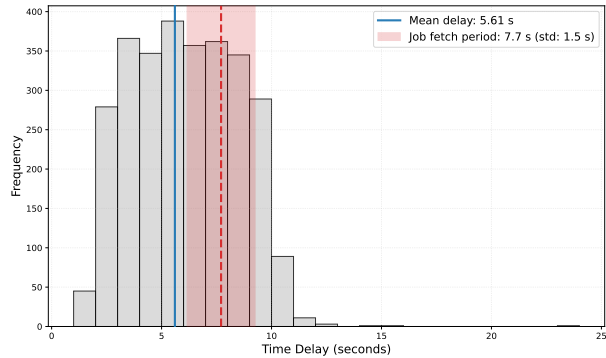


Fig. 5: Time delay distribution between Qubic block timestamps and job fetch timestamps. The mean delay is 5.61 seconds, and the green line marks the near 8-second job fetch period.

with a strategy of mining blocks early and selectively withholding them prior to broadcast. While a minor subset of Qubic blocks displays anomalously high timestamps, these outliers are predominantly associated with orphaned blocks.

Furthermore, to verify timestamp integrity, we measured the time difference between the block’s timestamp and the timestamp of the preceding job fetch response recorded locally (Fig. 5). The mining client is configured to fetch new jobs approximately every 7 seconds, though the actual average period was recorded as 7.7 seconds due to response delays and network circumstances. Consequently, the observed mean delay of 5.61 seconds falls naturally within this effective fetch interval, representing the expected time elapsed between receiving a job and finding a valid nonce. This alignment indicates that the timestamps are a natural byproduct of the mining workflow rather than the result of deliberate falsification. Consequently, we find no compelling evidence of large-scale timestamp manipulation that would invalidate temporal reasoning regarding Qubic’s behavior.

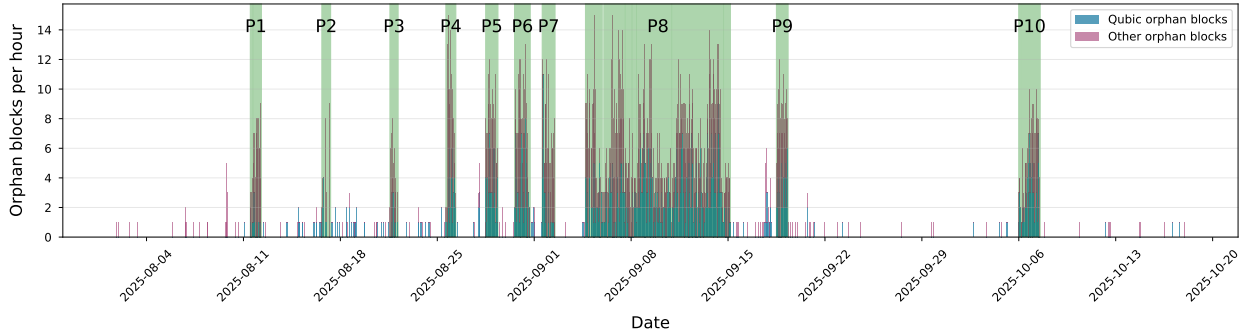


Fig. 6: Orphan block frequency and selfish mining periods

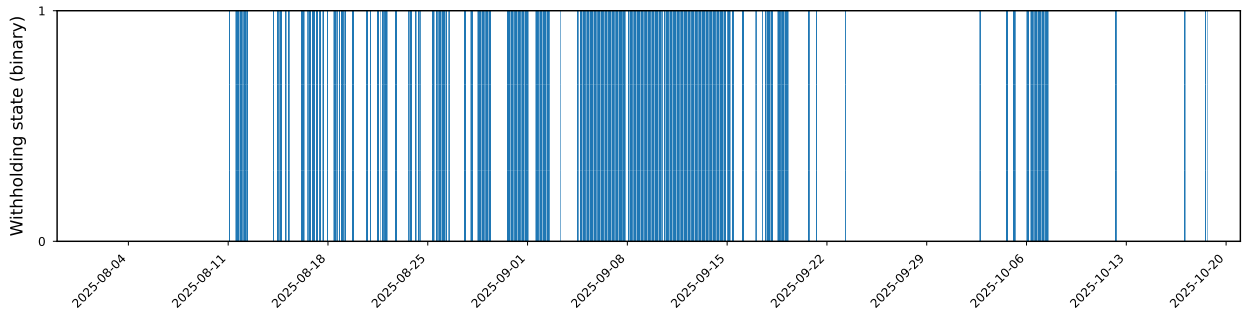


Fig. 7: Binary Qubic Block Withholding-Activity Timeline

In light of these observations, we treat Qubic’s timestamps as a sufficiently reliable proxy for inferring the relative ordering of events and for detecting patterns indicative of selfish mining. Specifically, we premise our analysis on the assumption that Qubic does not consistently alter timestamps to obfuscate private chain lead lengths or release decisions. Leveraging this assumption, we subsequently utilize orphan dynamics and timestamp data to illustrate the specific time intervals in which selfish mining was likely active. Additionally, community packet-level observations reported millisecond-level alignment between task issuance and reception, consistent with our conclusion that large-scale timestamp manipulation is unlikely.

### C. Selfish mining period categorization

Qubic’s strategy may vary over time, and selfish mining, if present, is unlikely to be applied uniformly across the entire observation window. To focus our analysis on intervals with meaningful deviations, we define a heuristic as Alg. 1 to identify periods with sustained abnormal orphan activity, which serves as an indicator of potential selfish mining.

The heuristic operates in three steps. First, we aggregate all orphan blocks (both Qubic and non-Qubic) into hourly bins and compute the orphan count  $C[h]$  for each hour. Second, we identify contiguous segments in which

---

#### Algorithm 1 Selfish Mining Period Heuristic

---

**Require:** Blocks  $B$  with timestamps and orphan flags, thresholds  $\tau_{\min}$ ,  $d_{\min}$ ,  $g_{\max}$

**Ensure:** Valid period spans  $M$

- 1: **Step 1:** Aggregate orphan blocks (Qubic + Other) by hour
  - 2:  $C[h] \leftarrow |\{b \in B : b.is\_orphan \wedge [b.timestamp]_{\text{hour}} = h\}|$
  - 3: **Step 2:** Find contiguous segments where each hour meets threshold
  - 4:  $S \leftarrow \{(s_i, e_i) : \forall h \in [s_i, e_i], C[h] \geq \tau_{\min} \wedge |e_i - s_i| \geq d_{\min}\}$
  - 5: **Step 3:** Merge segments with gaps  $\leq g_{\max}$  hours
  - 6:  $M \leftarrow \text{merge}(S, g_{\max})$
  - 7: **return**  $M$
- 

every hour satisfies a minimum orphan-count threshold  $\tau_{\min}$  and the total segment length exceeds a minimum duration  $d_{\min}$ . Third, we merge neighboring segments separated by gaps shorter than  $g_{\max}$  hours to tolerate brief fluctuations in activity. The result is a set  $M$  of candidate selfish mining periods.

In our evaluation, we set  $\tau_{\min} = 2$  orphan blocks per hour,  $d_{\min} = 4$  hours, and  $g_{\max} = 6$  hours. These parameters were chosen to capture intervals where elevated orphan activity is persistent enough to be unlikely under

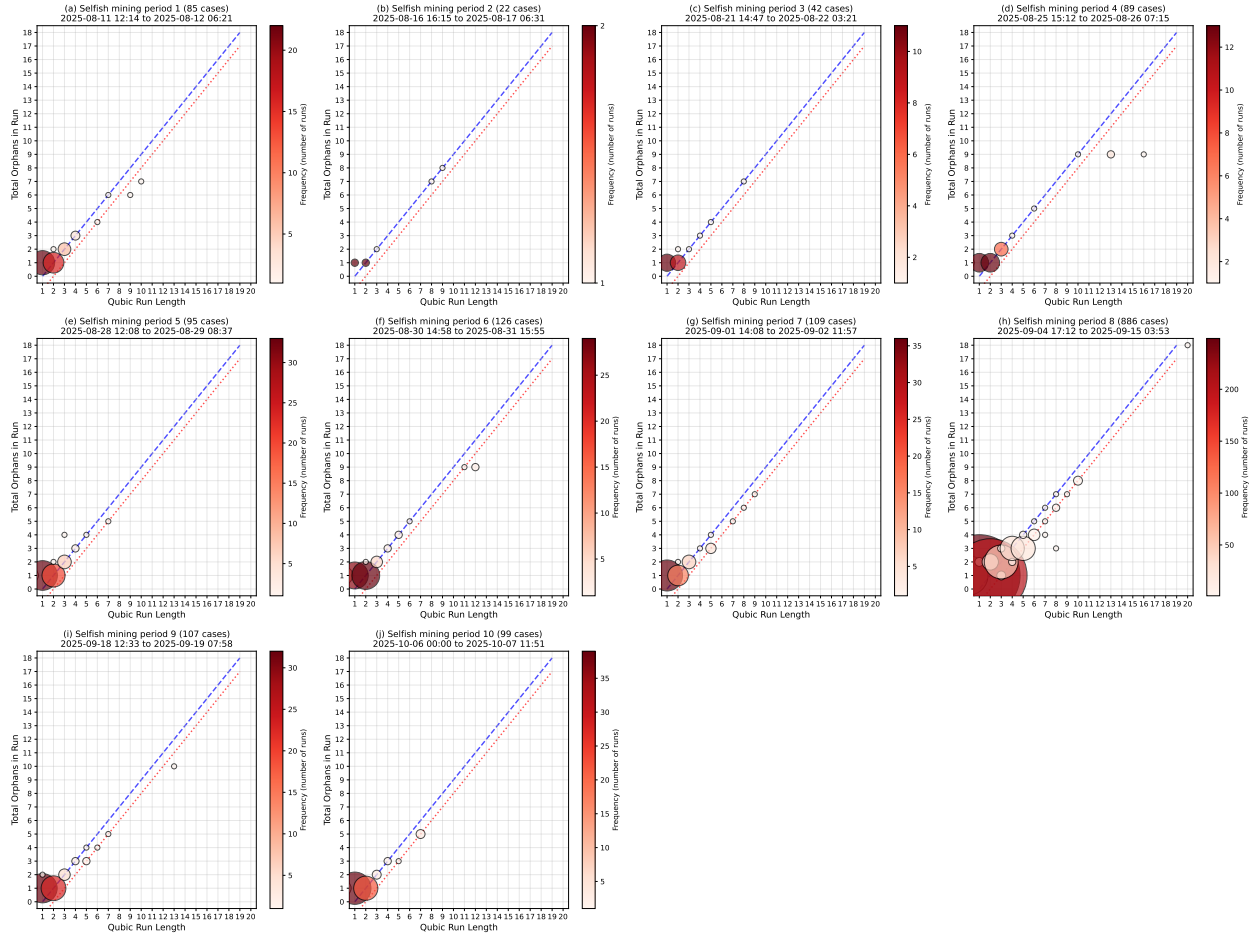


Fig. 8: Distribution of orphan blocks per Qubic run length across ten selfish mining periods (a-j). The scatter plots visualize run frequency (encoded by point size and color) for each run length and orphan count pair. Reference lines include the theoretical ideal selfish mining line  $y = x - 1$  (blue dashed) and the secondary threshold  $y = x - 2$  (red dotted).

normal conditions, while avoiding over-fragmentation due to minor gaps. Fig. 6 shows the resulting candidate periods on the timeline. Applying this heuristic yields ten periods (P1–P10) during which Qubic’s block share and involvement in orphan blocks are noticeably higher than their global averages, suggesting that Qubic concentrated its selfish mining behavior in these windows. In particular, Qubic’s average hashrate share in these periods is 28.02%, higher than its overall share of 22.09%. This gap indicates that Qubic tends to enable selfish mining only after its hashrate reaches a comparatively high level, and to cease such behavior once its effective share falls back toward the baseline.

Using the measured  $\alpha = 28.02\%$  for the selfish mining periods together with the observed low  $\gamma \approx 0$ , we evaluate both the classical selfish mining revenue function and the derived modified-strategy revenue.

Fig. 8 further illustrates how Qubic’s behavior varies

across the identified periods by plotting the lengths of Qubic-controlled runs against the number of associated orphan blocks. In early periods (P1–P4), most points lie close to the reference blue line ( $y = x - 1$ ) corresponding to releasing the private chain at lead 1, which is broadly consistent with the classical selfish mining strategy that maximizes the waste of the other mining power. In contrast, during P8, where Qubic’s activity is most intensive, we observe many runs aligned with patterns indicative of releasing at lead 2, suggesting a more conservative policy that avoids exposing the pool to tie situations when the lead is only one block. This shift supports the view that Qubic adapts its release rule depending on its effective hashrate and perceived network conditions, motivating the need for an analytical model that explicitly captures such a modified strategy.

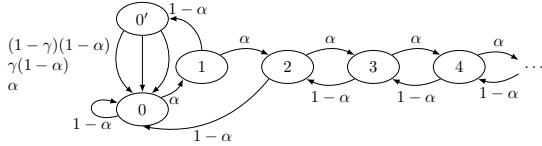


Fig. 9: State machine of the original selfish mining.

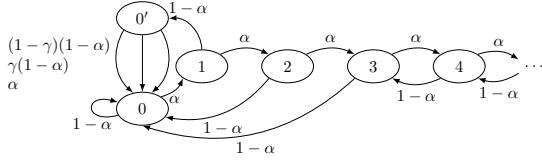


Fig. 10: State machine of a modified selfish mining model with a modified transition from state 3 to 0.

#### D. Analytical model of Qubic's selfish mining behavior

To interpret the observed periods, we compare them against analytical models of selfish mining. We first recall the classical selfish mining revenue function  $R_{\text{selfish}}(\alpha, \gamma)$ , which expresses the pool's expected revenue share as a function of its relative hashrate  $\alpha$  and the network tie-breaking parameter  $\gamma$ . Its revenue can be calculated based on the state machine depicted in Fig. 9. Each state presents *lead* denotes the number of blocks by which the selfish miner is ahead. For example, if a selfish miner's private chain has height 103 and the honest miners' public chain has height 100, then the system's state is 3. State  $0'$  corresponds to the situation where the selfish miner has mined a block first and the honest miners have also mined a competing block, so the network is in a tie-breaking state. The tie can be resolved in three ways: (1) an honest miner extends the honest chain with probability  $(1-\alpha)(1-\gamma)$ ; (2) an honest miner extends the selfish miner's chain with probability  $(1-\alpha)\gamma$ ; or (3) the selfish miner extends the selfish miner's own chain with probability  $\alpha$ . Eq. 1 gives the revenue of the selfish mining [1].

$$R_{\text{selfish}}(\alpha, \gamma) = \frac{\alpha(1-\alpha)^2(4\alpha + \gamma(1-2\alpha)) - \alpha^3}{1-\alpha(1+(2-\alpha)\alpha)} \quad (1)$$

We then consider a slightly different selfish mining strategy. Fig. 10 represents a modified strategy motivated by Qubic's observed behavior, in which the private chain is frequently released at lead 2 and includes an additional transition pattern (e.g., from state 3 to 0) reflecting more conservative release decisions. Qubic's overall strategy is best understood as lying between these two models rather than matching either one exactly.

Using this model, we derive a closed-form expression for the expected revenue of the modified strategy as a function of  $\alpha$  and  $\gamma$ .

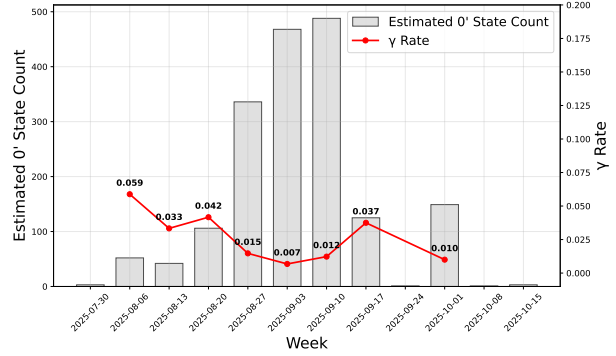


Fig. 11: Weekly  $\gamma$  rate and estimated state  $0'$  counts

**Theorem 1.** Let  $R_{\text{mod}}(\alpha, \gamma)$  denote the selfish pool's long-run fraction of accepted blocks under the modified strategy encoded by the state machine in Fig. 10, where  $\alpha \in (0, \frac{1}{2})$  is the pool's relative hash power and  $\gamma \in [0, 1]$  is the tie-breaking parameter. Then

$$R_{\text{mod}}(\alpha, \gamma) = \frac{\alpha(\alpha^3\gamma - 3\alpha^2\gamma + \alpha^2 + 3\alpha\gamma - 2\alpha - \gamma)}{\alpha^4 - 2\alpha^3 + \alpha - 1} \quad (2)$$

*Proof.* See Appendix A.  $\square$

#### E. Expected revenue under observed parameters

We now apply the analytical model using parameters inferred from the identified selfish-mining periods. For each period, we estimate Qubic's relative hashrate  $\alpha$  from its share of main-chain and orphaned blocks, and derive an empirical tie-breaking parameter  $\gamma$  by counting events in which Qubic and non-Qubic blocks compete at the same height and observing which block is eventually adopted. Fig. 11 shows that the weekly estimates of  $\gamma$  are close to zero. We attribute this to delayed propagation of Qubic blocks: although their timestamps are earlier, they tend to arrive at nodes later.

For the relevant range of  $\alpha$  and the near-zero  $\gamma$  observed in our data, both the standard and modified selfish mining models predict that Qubic's expected revenue is not superior to that of honest mining as Fig. 12 illustrates. At the average hashrate share of 28.02% during the identified selfish mining periods and  $\gamma \approx 0$ , the standard selfish mining model yields an expected revenue ratio of  $R_{\text{selfish}} \approx 25.53\%$ , while the modified model yields  $R_{\text{mod}} \approx 17.82\%$ . Since Qubic's actual strategy is best understood as lying between these two models, its expected revenue ratio should also fall within this interval, implying a relative loss of roughly 9% – 36% compared to honest mining at the same hashrate.

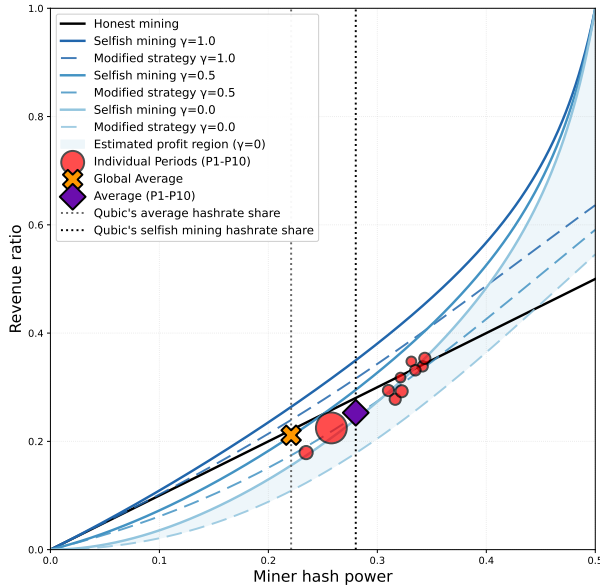


Fig. 12: Theoretical selfish mining revenues and observed Qubic’s mining revenue by periods, average of period, and the global average. The light-blue shaded area denotes the theoretically predicted revenue range when  $\gamma = 0$ .

These results indicate that, under realistic network conditions, Qubic’s selfish mining behavior would not provide a mining reward advantage and is, from a narrow revenue perspective, irrational.

#### F. Comparing the theoretic expectation and observed revenue

Again in Fig. 12, we presented the observed revenue of Qubic with categorizing the global average, the selfish period mining average, and each selfish mining period’s average. Table III shows the detailed numbers. Unlike our theoretic expectation, the Qubic’s revenue did not approach the lower bound (the modified selfish mining). Rather, the Qubic sometimes outperformed the lower bound of the normal selfish mining. And P6 and P9 outperformed the honest mining revenue even though the selfish mining average and the global average underperformed the honest mining. In the next section, we analyze this difference.

### VI. ANALYSIS ON DIFFERENCE BETWEEN REVENUE EXPECTATION BY THEORY AND OBSERVATION

In this section, we analyze the discrepancy between the theoretical revenue expectations derived from our models and the actual observed revenue of the Qubic pool during the identified selfish mining periods. We then provide a conjecture regarding the underlying causes of this divergence.

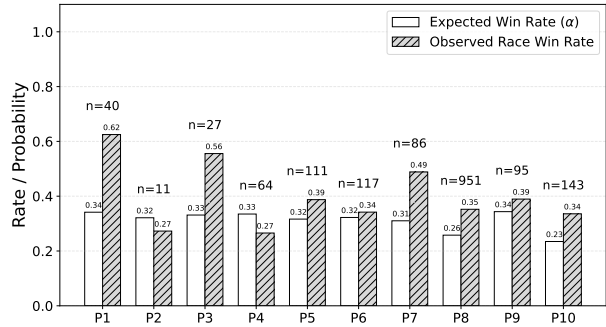


Fig. 13: Qubic’s winning ratio at State  $0'$

#### A. Tie-breaking winning rate

To understand the deviation observed in Fig. 12, we initially hypothesized that the empirically derived tie-breaking parameter  $\gamma$  might have been underestimated in our previous analysis. However, a closer inspection revealed that the primary anomaly lay not in the global  $\gamma$  estimation, but in the specific winning rate of Qubic at state  $0'$ —the scenario where a selfish miner competes in single block race against the rest of the network.

As illustrated in Fig. 13, Qubic’s winning rate in these race conditions was consistently higher than its estimated mining power ( $\alpha$ ) for most periods, with the exceptions of P2 and P4. Notably, several periods exhibited a race winning rate that significantly exceeded the corresponding hashrate share. For instance, in period P1, the observed winning rate was 0.62 against an  $\alpha$  of 0.34. Similarly, P3 showed a rate of 0.56 (vs.  $\alpha = 0.33$ ), and P7 showed 0.49 (vs.  $\alpha = 0.31$ ).

#### B. Temporal granularity of selfish mining identification

We considered several possibilities to explain why the observed behavior deviated from the theoretical models. The most plausible explanation is that the heuristic periods identified by Algorithm 1 were too rough, inadvertently capturing intervals where selfish mining was not actively employed. While our heuristic defined periods based on a rough 4-hour threshold with 6-hour gaps, it is likely that Qubic dynamically toggled its selfish mining strategy on and off with much finer granularity, responding delicately to real-time fluctuations in its mining power which Qubic can estimate precisely.

This hypothesis is supported by the data from period P8, which offers a large sample size over a long duration. In P8, the average mining power share was measured at 25.78%, yet the tie-breaking winning rate at state  $0'$  was approximately 35%. We conjecture that 35% represents Qubic’s true effective hashrate during the brief sub-intervals when it was actively engaged in selfish mining. If we assume an active mining power of  $\alpha = 0.35$  with

$\gamma \approx 0$ , the theoretical revenue of selfish mining would be bounded between 36.65% (Eq. 1, upper bound) and 28.04% (Eq. 2, lower bound).

However, the actual observed revenue for P8 was only 22.48%. This suggests that even if Qubic attempted to execute the strategy, it failed to outperform honest mining. In relative terms, this corresponds to a revenue loss of approximately 12% compared to honest mining ( $\approx 25.78\%$ ). This significant underperformance implies that the strategy was not executed efficiently enough to overcome the inherent risks of selfish mining.

Conversely, in periods such as P1 and P3, Qubic did outperform honest mining. These periods were characterized by a high baseline mining power (30%–40%), and the exceptionally high race winning rates (Fig. 13) suggest that Qubic’s effective power was dominant during the specific moments of attack. Nevertheless, the excess revenue gained over honest mining was marginal—more or less than 5%—and these successful instances constituted only a minor fraction of the total observation timeline.

Our overall analysis indicates that Qubic’s selfish mining campaign was, on aggregate, inefficient and failed to consistently outperform honest mining. The measured revenue often fell below the theoretical profitability threshold, likely due to the difficulty of maintaining optimal strategy execution under real-world network variance. However, despite the lack of financial success for the attacker, the strategy induced severe negative externalities on the Monero network. The identified periods coincided with elevated orphan rates and significantly deeper chain reorganizations, degrading the effective reliability of transaction confirmations. This tension between the attacker’s private loss and the public harm inflicted on the network motivates the discussion of mitigation strategies in the subsequent sections.

## VII. TIME-VARYING RELATIVE HASHRATE AND INTERMITTENT SELFISH MINING

We highlighted a persistent gap between the profitability predicted by static selfish-mining models and the profitability observed in practice. One explicit reason is that the selfish mining was frequently and intermittently conducted as shown in Fig. 7, not consistently performed.

In real networks, both the pool hashrate and the total network hashrate fluctuate over time, so the attacker’s relative hashrate is naturally modeled as a time-varying process  $\alpha(t)$ . This suggests that, rather than committing to selfish mining continuously, an attacker may benefit from *switching* the strategy on and off across time intervals as the observed data demonstrate.

In this section, we introduce a minimal model for intermittent selfish mining under time-varying  $\alpha(t)$  and

show, under a standard difficulty-adjustment abstraction, that switching can strictly improve long-run average revenue.

### A. Model setup for time-varying relative hashrate and threshold switching

We consider discrete time indexed at a granularity fine enough to represent strategic decisions (e.g., per-block opportunity or a short time grid relative to the difficulty window). Let  $\alpha(t) \in (0, 1)$  denote the attacker’s relative hashrate at time  $t$ .

a) *Switching policy*: The attacker selects  $S(t) \in \{0, 1\}$ , where  $S(t) = 0$  denotes honest mining and  $S(t) = 1$  denotes selfish mining. We adopt a minimal threshold switching rule:

$$S(t) = \mathbb{I}\{\alpha(t) > \alpha_{\text{th}}\}, \quad (3)$$

where  $\alpha_{\text{th}}$  is the (static-model) profitability threshold for the given propagation parameter  $\gamma$ .

b) *Separating share and efficiency*: To avoid committing to a specific closed-form expression while retaining the core economics, we decompose selfish mining into two effects:

- Main-chain share function  $\rho(\alpha, \gamma)$ : the attacker’s expected share of *main-chain* blocks when selfish mining at relative hashrate  $\alpha$ .
- Main-chain efficiency function  $\eta(\alpha, \gamma)$ : the fraction of physical block production that contributes to main-chain growth under selfish mining at relative hashrate  $\alpha$ .

Under honest mining,  $\rho(\alpha, \gamma) = \alpha$  and  $\eta(\alpha, \gamma) = 1$ .

We assume the standard qualitative properties consistent with selfish-mining analyses:

- For  $\alpha > \alpha_{\text{th}}$ , selfish mining provides a local advantage in main-chain share:  $\rho(\alpha, \gamma) > \alpha$ .
- Selfish mining induces waste (orphans) and reduces efficiency:  $0 < \eta(\alpha, \gamma) < 1$  when  $S = 1$ .

### B. Difficulty adjustment as an averaging mechanism

Difficulty adjustment aggregates recent observations over a window and therefore attenuates short-term fluctuations in effective main-chain productivity. Informally, a long window behaves like an *averaging mechanism*: rapid variations in strategy and hashrate are smoothed out in the difficulty signal.

We adopt the following time-scale abstraction.

**Assumption 1** (Time-Scale Separation for Difficulty Adjustment Algorithm). *Let  $W$  denote the effective averaging window of the DAA. The fluctuations in  $\alpha(t)$  and the switching in  $S(t)$  occur on a time scale shorter than  $W$ , so that the difficulty reacts primarily to the window-average of main-chain efficiency.*

Under Assumption 1, the long-run revenue comparison can be expressed in terms of efficiency-weighted averages (formalized below). This assumption works well for Monero comparatively. Appendix A discusses the details.

### C. Average revenue under switching

Define the instantaneous main-chain share of the attacker as

$$q(t) = \begin{cases} \alpha(t), & \text{if } S(t) = 0, \\ \rho(\alpha(t), \gamma), & \text{if } S(t) = 1, \end{cases} \quad (4)$$

and the instantaneous main-chain efficiency as

$$\eta(t) = \begin{cases} 1, & \text{if } S(t) = 0, \\ \eta(\alpha(t), \gamma), & \text{if } S(t) = 1. \end{cases} \quad (5)$$

A standard steady-state abstraction under DAA averaging is that the attacker's long-run expected revenue share is well-approximated by an efficiency-weighted ratio:

$$\bar{R}_{\text{switch}} \approx \frac{\mathbb{E}[\eta(t)q(t)]}{\mathbb{E}[\eta(t)]}, \quad (6)$$

where the expectation is taken over time in the stationary regime. By contrast, under always-honest mining, the attacker's long-run share is

$$\bar{R}_{\text{honest}} = \mathbb{E}[\alpha(t)]. \quad (7)$$

### D. A sufficient condition for profitability below the static threshold

Let  $\mathcal{S} = \{t : \alpha(t) > \alpha_{\text{th}}\}$  denote the selfish interval under threshold switching, and let  $p = \Pr[t \in \mathcal{S}]$ . Define the conditional means

$$\begin{aligned} a_H &= \mathbb{E}[\alpha(t) \mid t \notin \mathcal{S}], \\ a_S &= \mathbb{E}[\alpha(t) \mid t \in \mathcal{S}], \\ e_S &= \mathbb{E}[\eta(\alpha(t), \gamma) \mid t \in \mathcal{S}], \\ r_S &= \mathbb{E}[\eta(\alpha(t), \gamma) \rho(\alpha(t), \gamma) \mid t \in \mathcal{S}]. \end{aligned} \quad (8)$$

Note that  $a_S > a_H$  by construction, and  $0 < e_S < 1$  whenever selfish mining induces waste.

**Proposition 1** (Intermittent Selfish Mining Can Be Profitable Below the Static Threshold). *Assume Assumption 1 and the revenue approximation (6). Under threshold switching  $S(t) = \mathbb{I}\{\alpha(t) > \alpha_{\text{th}}\}$ , the switching strategy yields strictly higher long-run revenue than always-honest mining if and only if*

$$r_S > \mathbb{E}[\alpha(t)]e_S + (1-p)(a_S - a_H). \quad (9)$$

*In particular, this inequality can hold even when  $\mathbb{E}[\alpha(t)] \leq \alpha_{\text{th}}$ , provided the efficiency-weighted selfish advantage in  $\mathcal{S}$  is large enough and the selfish interval is not too frequent.*

*Proof.* See Appendix A.  $\square$

## VIII. OPERATIONAL DYNAMICS

The previous sections focused on theoretical analysis; however, interpreting this campaign also requires operational considerations that are not captured by the model. This section therefore summarizes qualitative observations and context gathered from communications with Monero community across a mix of public and private channels. Because these exchanges span heterogeneous venues and are not consistently citable (e.g., private messages, ephemeral discussions, and scattered public threads), it is difficult to provide complete, verifiable references for each detail. Moreover, much of the information was collected opportunistically and is not preserved in a reproducible form, which limits independent replication. Accordingly, we treat these inputs as anecdotal evidence and use them only to support plausibility arguments. We have checked that the described behaviors are technically feasible and not inconsistent with publicly observable events and Qubic's publicly documented actions.

### A. Spying and leakage

To detect Qubic's private mining activity, the Monero community deployed monitoring nodes across the network. By connecting to Qubic's low-level mining network from multiple observation nodes, collecting packet-level data, and analyzing local logs, the monitoring infrastructure reconstructed the timing of mining jobs and their corresponding solution messages on the network of Computers, the validator computers that run Qubic's consensus [21].

Each job encodes a block template, a candidate block assembled for mining that specifies the header and the set of transactions, which allowed us to track which template Qubic used at a given time and when the corresponding solution was observed. Then the origin and integrity of the collected messages were validated by verifying the digital signatures of Qubic's dispatcher and *computer* nodes, and matched each job to its corresponding solution. Finally, the PoW hash in the Result field of each solution message was used to match solution messages to reconstructed Monero blocks. Timing was obtained from reception logs tagged with timestamps.

Using the nonce and `tx_extra` values extracted from solution messages, the Monero community incorporated them into the corresponding block template to reconstruct a candidate block. It then verified the reconstruction by checking whether the resulting PoW hash matched and attempted to propagate the block to the Monero network. The goal was to weaken Qubic's private mining strategy by publishing and relaying blocks it had mined privately before Qubic could reveal them, thereby limiting its ability to accumulate a private chain and gain a length advantage.

### B. Defense and counterattack

In response to these monitoring-based interventions, Qubic soon began to develop its countermeasures. First, to prevent leakage of mining-solution data, it introduced encryption for solution messages circulating on the network. Initially, Qubic applied a simple XOR-based scheme. However, solution messages contain fixed or easily inferable header fields, so we infer that the key could be recovered via known-plaintext analysis. As a result, the scheme was quickly broken by the Monero community. Qubic then iterated on its solution-encryption scheme by changing the method and keys multiple times, rotating keys regularly, and adjusting the protocol, including relaying messages through indirect paths, to make external monitoring increasingly difficult. These measures progressively reduced the community’s ability to extract critical information such as solutions in real time. Therefore, as long as Qubic maintained an open *computer*-network architecture, it was difficult to fully eliminate the possibility that external observers could conduct monitoring or limited intervention based on network traffic.

Under this constraint, Qubic strengthened operational measures to reduce information exposure, including encryption, key rotation, and changes to message-routing paths. Over time, they observed the network shift toward a more controlled and centralized configuration, with tighter control over task dissemination and increasing reliance on a small set of dispatching points.

As a more fundamental countermeasure, Qubic introduced a strategy that uses withheld transactions. These are transactions that are intentionally omitted from the block template shared on the network. They are revealed only when Qubic later publishes/relays the block, and are not included in the initially shared templates. This prevents external parties from fully reconstructing the underlying block template. This makes it difficult to reproduce an identical block header even if the nonce is recovered from a solution message, thereby limiting attempts to reconstruct a valid block from solution information alone and propagate it first.

After Qubic began using withheld transactions, early block publication became far less effective. The Monero community therefore shifted its response. Instead of relying on immediate propagation, the community reconstructed past blocks after Qubic later disclosed the missing transactions through other channels, and then published and relayed them to enable retrospective verification.

### C. Operational takeaways

This sequence shows that Qubic’s revenue advantage was not determined by hashrate dynamics alone. Because

the campaign was carried out through a public mining pool, the usual assumption that an attacker can reliably maintain a private chain was necessarily weakened. As a result, attack and defense progressed in parallel. Each move on one side prompted immediate operational changes on the other, and the attack strategy was repeatedly revised in response to these iterative exchanges.

These observations indicate that the campaign’s outcome was shaped by multiple interacting factors. In particular, it depended on whether block and solution information was exposed, how propagation occurred across the network, whether blocks could be reconstructed and disseminated, and how strategies evolved through iterative operation.

## IX. DISCUSSION

Our primary focus has been on analyzing Qubic’s selfish mining strategies. In this section, we turn to two technical defense approaches against the Qubic’s campaign in the Monero community. The first approach is to modify the main-chain selection rule so that nodes are less likely to accept blocks produced by a selfish miner. The second is *detective mining*, which mitigates deep private selfish chains without any modification to the chain-selection rules.

### A. Chain-selection rule modification

A natural class of countermeasures against selfish mining is to modify the chain-selection rule so that withheld blocks become less valuable to an attacker. Existing proposals along this line include timestamp- and freshness-based fork-choice rules and backward-compatible schemes such as Publish or Perish [13]–[15]. These mechanisms typically penalize blocks that propagate too slowly or reward chains that incorporate more timely blocks and uncles, thereby reducing the benefit of maintaining a long private chain [16], [17].

Following Qubic’s campaign, parts of the Monero community actively discussed adopting a Publish-or-Perish-style rule [19]. However, such approaches rely on relatively strong assumptions about network-wide propagation bounds and timing information, which are difficult to guarantee in a heterogeneous, permissionless environment like Monero. Moreover, deploying a new chain-selection rule at this point would mainly protect against future selfish mining attempts rather than mitigating the damage from Qubic’s already finished campaign.

More broadly, our case study reinforces a well-known limitation of proof-of-work systems: when the overall hash power is modest and concentrated, the system remains structurally exposed to selfish mining and related strategies. This tension has motivated some ecosystems to explore alternatives such as proof-of-stake or hybrid

designs. While a full evaluation of such alternatives is beyond the scope of this work, our findings suggest that Monero must either secure a sufficiently large and decentralized mining power or eventually confront this design trade-off.

### B. Detective mining and its limitation

In contrast to protocol-level modifications, the Monero community highlighted *detective mining* as a countermeasure that does not require any modification to the chain-selection rules [18]. One characteristic of Qubic’s selfish mining attack is that it is carried out by a public mining pool. Detective mining has been studied under the assumption that a public mining pool performs selfish mining [22]. Because the selfish mining pool is public, some information about its private chain is partially observable to miners. In particular, the previous Merkle root, which is essential for tracking the private chain, is visible. Rational miners may then prefer to mine on the leading private chain rather than on the lagging public chain. In theory, such miners obtain a higher expected reward than both the selfish miner and honest miners.

However, this approach raises two issues. The first is the possibility of a Denial-of-Service (DoS) attack by the selfish mining pool. Detective miners do not know the transactions contained in the previous private blocks, and if the selfish mining pool refuses to release its private blocks after a detective-mining block is found, miners are unable to include transactions on the longest chain. The second issue is that some community members objected to the idea of miners intentionally building on the selfish miner’s private chain. Moreover, detective mining further accelerates the loss incurred by honest miners.

## X. CONCLUSION

This paper provides an empirical analysis of Qubic’s selfish-mining campaign on Monero. We reconstruct the campaign using a Monero pruning node, public nodes, and the Qubic pool API, and identify intervals consistent with selfish mining behavior. Qubic’s observed share rose to 23–34% but never sustained majority control. Comparing measurements against the classical model and a campaign-informed variant, we find profitability to be fragile overall, yet the campaign substantially increased orphaning and reorganization depth, degrading confirmation reliability. Finally, we explain gaps between static predictions and observations using time-varying relative hashrate and operational frictions, and show that intermittent switching during favorable intervals can improve long-run revenue under certain conditions even when the time-average hashrate is below the classical threshold. This highlights the need for monitoring and mitigations that account for adaptive, interval-based attacks, not only sustained majority attempts.

## ACKNOWLEDGEMENT

We are grateful to the Monero community for sharing artifacts and empirical observations that complemented our measurements. We especially thank two contributors, DataHoarder (<https://github.com/WeebDataHoarder>) and Sergei Chernykh (sech1) for providing access to supplemental datasets and for answering technical questions that helped us validate and refine parts of our analysis. Also, we appreciate discussion from Yunkyu Lee and Huiwoo Kim.

## REFERENCES

- [1] I. Eyal and E. G. Sirer, “Majority is not enough: Bitcoin mining is vulnerable,” *Communications of the ACM*, vol. 61, no. 7, pp. 95–102, 2018.
- [2] retrodrive, “Qubic performs 51% monero network takeover demonstration,” <https://qubic.org/blog-detail/historic-takeover-complete-qubic-miners-now-secure-monero-network>, Aug. 2025, accessed: 2025-10-25.
- [3] —, “Epoch 172 recap - the monero experiment,” <https://qubic.org/blog-detail/epoch-172-recap-the-monero-experiment>, Aug. 2025, accessed: 2025-10-25.
- [4] K. Nayak, S. Kumar, A. Miller, and E. Shi, “Stubborn mining: Generalizing selfish mining and combining with an eclipse attack,” in *IEEE European Symposium on Security and Privacy (EuroS&P)*. IEEE, 2016, pp. 305–320. [Online]. Available: <https://doi.org/10.1109/EUROSP.2016.32>
- [5] A. Sapirshtein, Y. Sompolinsky, and A. Zohar, “Optimal selfish mining strategies in bitcoin,” in *International conference on financial cryptography and data security*. Springer, 2016, pp. 515–532.
- [6] R. B. Zur, I. Eyal, and A. Tamar, “Efficient MDP analysis for selfish-mining in blockchains,” in *Proceedings of the 2nd ACM Conference on Advances in Financial Technologies (AFT)*. ACM, 2020, pp. 113–131. [Online]. Available: <https://doi.org/10.1145/3419614.3423264>
- [7] C. Feng and J. Niu, “Selfish mining in ethereum,” in *IEEE 39th International Conference on Distributed Computing Systems (ICDCS)*. IEEE, 2019, pp. 1306–1316. [Online]. Available: <https://doi.org/10.1109/ICDCS.2019.00131>
- [8] S.-N. Li, C. Campajola, and C. J. Tessone, “Statistical detection of selfish mining in proof-of-work blockchain systems,” *Scientific Reports*, vol. 14, no. 1, p. 6251, 2024. [Online]. Available: <https://www.nature.com/articles/s41598-024-55348-3>
- [9] C. Decker and R. Wattenhofer, “Information propagation in the bitcoin network,” in *13th IEEE International Conference on Peer-to-Peer Computing (P2P)*, September 2013.
- [10] J. Fechner, B. Chandrasekaran, and M. X. Makkes, “Calibrating the performance and security of blockchains via information propagation delays: revisiting an old approach with a new perspective,” in *Proceedings of the 37th ACM/SIGAPP Symposium on Applied Computing (SAC ’22)*. ACM, 2022, pp. 282–289. [Online]. Available: <https://doi.org/10.1145/3477314.3507003>
- [11] R. Shi, Z. Peng, L. Lan, Y. Ge, P. Liu, Q. Wang, and J. Wang, “Eclipse attacks on monero’s peer-to-peer network,” in *Network and Distributed System Security Symposium (NDSS)*, 2025. [Online]. Available: <https://www.ndss-symposium.org/wp-content/uploads/2025-95-paper.pdf>
- [12] D. I. Ilie, S. M. Werner, I. Stewart, and W. J. Knottenbelt, “Unstable throughput: When the difficulty algorithm breaks,” *CoRR*, vol. abs/2006.03044, 2020. [Online]. Available: <http://arxiv.org/abs/2006.03044>
- [13] E. Heilman, “One weird trick to stop selfish miners: Fresh bitcoins, a solution for the honest miner,” in *International Conference on Financial Cryptography and Data Security*. Springer, 2014, pp. 161–162.

- [14] S. Solat and M. Potop-Butucaru, “Brief announcement: Zeroblock: Timestamp-free prevention of block-withholding attack in bitcoin,” in *International Symposium on Stabilization, Safety, and Security of Distributed Systems*. Springer, 2017, pp. 356–360.
- [15] R. Zhang and B. Preneel, “Publish or perish: A backward-compatible defense against selfish mining in bitcoin,” in *Cryptographers’ Track at the RSA Conference*. Springer, 2017, pp. 277–292.
- [16] R. Pass and E. Shi, “Fruitchains: A fair blockchain,” in *Proceedings of the ACM symposium on principles of distributed computing*, 2017, pp. 315–324.
- [17] P. Szalachowski, D. Reijnders, I. Homoliak, and S. Sun, “{StrongChain}: Transparent and collaborative {Proof-of-Work} consensus,” in *28th USENIX Security Symposium (USENIX Security 19)*, 2019, pp. 819–836.
- [18] R. Spagni, “(github issue #140) implement detective mining (pool software change, no protocol change required),” <https://github.com/monero-project/research-lab/issues/140>, Aug. 2025, accessed: 2025-10-25.
- [19] tevador, “(github issue #144) selfish mining mitigations (publish or perish),” <https://github.com/monero-project/research-lab/issues/144>, Aug. 2025, accessed: 2025-10-25.
- [20] D. A. Wijaya, J. K. Liu, R. Steinfeld, and D. Liu, “Transparency or anonymity leak: Monero mining pools data publication,” in *Information Security and Privacy (ACISP 2021)*, ser. Lecture Notes in Computer Science. Springer, 2021. [Online]. Available: [https://dl.acm.org/doi/10.1007/978-3-030-90567-5\\_22](https://dl.acm.org/doi/10.1007/978-3-030-90567-5_22)
- [21] Qubic Docs. Node types in the qubic network. [Online]. Available: <https://docs.qubic.org/learn/nodes/>
- [22] S. Lee and S. Kim, “Rethinking selfish mining under pooled mining,” *ICT Express*, vol. 9, no. 3, pp. 356–361, 2023.

## APPENDIX

The dataset and scripts to reproduce our analyses and figures are available at <https://github.com/shlee-lab/Qubic-selfish-mining-study>.

Listing 1: Qubic extra-nonce regex patterns

```
# Pattern A
([0-9a-f]{4})0000([0-9a-f]{8})([0-9a-f]{8})0{10}
# Pattern B
([0-9a-f]{4})0100([0-9a-f]{8})([0-9a-f]{8})0{10}
# Pattern C
01([0-9a-f]{16})
```

*Proof.* We derive the stationary distribution of the Markov chain in Fig. 10 and then compute the expected rewards per block-finding event.

Let  $\pi_s$  be the stationary probability of state  $s$ . From Fig. 10 we read off the following balance equations.

*a) Tie state:* From state 1, an honest block (probability  $1 - \alpha$ ) leads to  $0'$ , and from  $0'$  the next block always resolves the fork and returns to 0. Thus

$$\pi_{0'} = (1 - \alpha)\pi_1. \quad (10)$$

*b) Lead 1 and 2:* From the transitions  $0 \rightarrow 1$  with probability  $\alpha$  and  $2 \rightarrow 1$  with probability  $1 - \alpha$ , and the outgoing probability 1 from state 1, we obtain

$$\pi_1 = \alpha\pi_0 + (1 - \alpha)\pi_2. \quad (11)$$

From  $1 \rightarrow 2$  with probability  $\alpha$  and total outflow 1 from state 2,

$$\pi_2 = \alpha\pi_1. \quad (12)$$

*c) Lead  $\geq 3$  (geometric tail):* For  $i \geq 3$  the figure shows: on a selfish block ( $\alpha$ ) the lead increases by one, and on an honest block ( $1 - \alpha$ ) the selfish miner publishes its private chain and the process returns to 0. Thus for  $i \geq 3$  we have pure geometric growth:

$$\pi_i = \alpha\pi_{i-1} \quad (i \geq 3), \quad (13)$$

hence  $\pi_i = \alpha^{i-2}\pi_2$  for all  $i \geq 2$ .

*d) State 0:* Incoming probability flow into 0 comes from: (i) the self-loop at 0 when an honest block is found, (ii) resolution of  $0'$ , (iii) full publication from any  $i \geq 3$  after an honest block. The balance for state 0 is therefore

$$\pi_0 = (1 - \alpha)\pi_0 + \pi_{0'} + (1 - \alpha) \sum_{i=3}^{\infty} \pi_i. \quad (14)$$

*e) Solving for  $\pi_s$ :* Using (12) and (13) we obtain

$$\pi_2 = \alpha\pi_1, \quad \pi_i = \alpha^{i-1}\pi_1 \quad (i \geq 2).$$

Substituting into (11) gives

$$\pi_1 = \alpha\pi_0 + (1 - \alpha)\alpha\pi_1 \quad \Rightarrow \quad \pi_1 = \frac{\alpha}{\alpha^2 - \alpha + 1} \pi_0.$$

Then

$$\pi_2 = \frac{\alpha^2}{\alpha^2 - \alpha + 1} \pi_0, \quad \pi_i = \frac{\alpha^i}{\alpha^2 - \alpha + 1} \pi_0 \quad (i \geq 2),$$

and from (10),

$$\pi_{0'} = (1 - \alpha)\pi_1 = \frac{\alpha(1 - \alpha)}{\alpha^2 - \alpha + 1} \pi_0.$$

Using (14) and the geometric sum  $\sum_{i=3}^{\infty} \alpha^i = \alpha^3/(1 - \alpha)$ , one checks that the balance holds with these expressions. Normalization

$$\pi_0 + \pi_{0'} + \sum_{i=1}^{\infty} \pi_i = 1$$

then yields

$$\pi_0 = 1 - 2\alpha + 2\alpha^2 - \alpha^3,$$

and thus all  $\pi_s$  are uniquely determined.

f) *Expected rewards:* We next compute the expected number of accepted blocks per block-finding event for the attacker ( $E_s$ ) and for the whole network ( $E_t$ ).

- In state 0, an honest block (probability  $1 - \alpha$ ) adds one accepted block for honest miners:

$$E_s^{(0)} = 0, \quad E_t^{(0)} = (1 - \alpha)\pi_0.$$

- In state  $0'$ , the next block always resolves the fork and finalizes two blocks. As in the original analysis, the attacker's expected share is  $2\alpha + \gamma(1 - \alpha)$ , so

$$E_s^{(0')} = \pi_{0'}(2\alpha + \gamma(1 - \alpha)), \quad E_t^{(0')} = 2\pi_{0'}.$$

- In states 1 and 2, one step does not finalize any block, only changes the lead, hence

$$E_s^{(1)} = E_s^{(2)} = 0, \quad E_t^{(1)} = E_t^{(2)} = 0.$$

- In each state  $i \geq 3$ , an honest block (probability  $1 - \alpha$ ) triggers full publication of the private chain: all  $i$  blocks are accepted for the attacker and the chain returns to 0. Therefore

$$E_s^{(i)} = (1 - \alpha)i\pi_i, \quad E_t^{(i)} = (1 - \alpha)i\pi_i.$$

Summing all contributions,

$$E_s = \pi_{0'}(2\alpha + \gamma(1 - \alpha)) + (1 - \alpha) \sum_{i=3}^{\infty} i\pi_i,$$

$$E_t = (1 - \alpha)\pi_0 + 2\pi_{0'} + (1 - \alpha) \sum_{i=3}^{\infty} i\pi_i.$$

Using the geometric series derivative formula  $\sum_{i=3}^{\infty} i\alpha^i = \alpha^3(3 - 2\alpha)/(1 - \alpha)^2$ , we evaluate the summation terms.

Crucially, we observe that the normalization constant  $\pi_0$  factorizes as:

$$\pi_0 = 1 - 2\alpha + 2\alpha^2 - \alpha^3 = (1 - \alpha)(\alpha^2 - \alpha + 1).$$

This factorization allows us to simplify the stationary probabilities:

$$\frac{\pi_0}{\alpha^2 - \alpha + 1} = 1 - \alpha.$$

Substituting this into the expressions for  $\pi_{0'}$  and  $\pi_i$ , the common denominator cancels out:

$$\begin{aligned} \pi_{0'} &= \alpha(1 - \alpha)(1 - \alpha) = \alpha(1 - \alpha)^2, \\ \pi_i &= \alpha^i(1 - \alpha) \quad (i \geq 2). \end{aligned}$$

Now, we substitute these simplified probabilities into the reward equations. For  $E_s$ :

$$\begin{aligned} E_s &= \pi_{0'}(2\alpha + \gamma(1 - \alpha)) + (1 - \alpha) \sum_{i=3}^{\infty} i\pi_i \\ &= \alpha(1 - \alpha)^2(2\alpha + \gamma(1 - \alpha)) + (1 - \alpha)^2 \sum_{i=3}^{\infty} i\alpha^i \\ &= \alpha(1 - \alpha)^2(2\alpha + \gamma(1 - \alpha)) + (1 - \alpha)^2 \frac{\alpha^3(3 - 2\alpha)}{(1 - \alpha)^2} \\ &= \alpha(1 - \alpha)^2(2\alpha + \gamma - \alpha\gamma) + \alpha^3(3 - 2\alpha). \end{aligned}$$

Expanding and collecting terms yields the final polynomial form:

$$E_s = -\alpha(\alpha^3\gamma - 3\alpha^2\gamma + \alpha^2 + 3\alpha\gamma - 2\alpha - \gamma).$$

Similarly for  $E_t$ :

$$\begin{aligned} E_t &= (1 - \alpha)\pi_0 + 2\pi_{0'} + (1 - \alpha) \sum_{i=3}^{\infty} i\pi_i \\ &= (1 - \alpha)^2(\alpha^2 - \alpha + 1) + 2\alpha(1 - \alpha)^2 + \alpha^3(3 - 2\alpha). \end{aligned}$$

Simplifying this expression leads to:

$$E_t = -(\alpha^4 - 2\alpha^3 + \alpha - 1).$$

Hence the attacker's long-run revenue ratio is

$$R_{\text{mod}}(\alpha, \gamma) = \frac{E_s}{E_t},$$

which is exactly Eq. 2.  $\square$

The view keys listed in Table II were obtained from the official Qubic Discord server (Accessible via <https://qubic.org/>), specifically from the disclosures made by Qubic's lead dev *dkat*. These keys are provided to enable the community to retrospectively verify the ownership and provenance of Qubic-mined blocks.

This time-scale issue differs across protocols. In Bitcoin, difficulty adjustments occur over long epochs (2016 blocks; 2 weeks), so the averaging window is large. An attacker who reduces main-chain efficiency via selfish mining may need to absorb the revenue impact for a long duration before difficulty responds, which can make intermittent attacks less attractive unless the attacker is willing to tolerate extended shortfall. In contrast, Monero-style designs that update difficulty frequently using a sliding-window estimator respond much more quickly to changes in effective productivity. In such systems, the loss-bearing interval before difficulty reacts can be shorter, making intermittent strategies that concentrate selfish mining in favorable sub-intervals more plausible.

Write the numerator and denominator in (6) by conditioning on  $\mathcal{S}$ .

On  $t \notin \mathcal{S}$ , we have  $\eta(t) = 1$  and  $q(t) = \alpha(t)$ , hence

$$\mathbb{E}[\eta(t)q(t) \mid t \notin \mathcal{S}] = \mathbb{E}[\alpha(t) \mid t \notin \mathcal{S}] = a_H. \quad (15)$$

TABLE II: Cubic View Key List

Date	Address	View Key	Note
May 27, 2025	47hhGMKbWpKfxDiqcejWGicVvQHEYd45AEaUyKVjczZ ywL8c8mtjN3oACGfdrsLrPGP2r49gvTBnBiTVQcEkf BNFEKCDy7ME	577fd4a7278f55d2a9230d32823b81497b2e854d4a 8702b1256a17cda42a760d	
Aug. 6, 2025	43oMtdwB5aaCuM9vVaiY6u7XgxCGLwA563C7b5V3oS TSjDdhiBkWeGxeZZSuD4wAydMzbvNwrF9iRGmwoMnh YnMTMcZjBrv	e935552c5665117a6ecc9fbbfd4156595c75774014 606130a01003720e063201	epoch 172
Aug. 13, 2025	49upGQgCYzxMKfBU9hYe8QH3fQQMSdReiAJx3vo9bq 6K4YegbgP39rVKNNGh9tA3VobYMkyGxvDc1J9FnVfW 8f4UT7BsDhf	0b21ef509769c6d95899cca7ccd86b89333ca4ce0d fa3fd5aa304059aed0f903	epoch 173
Aug. 20, 2025	4AqzG7scWP19yNsFuJNpQ2CNF7LGxJNTJaEennAA48 KbLX6a7PTazW4c3FTwBPfjJ4TFq3xpZhvGvgygVCT uXxSLWrAk3S	05ada241eea8b262241762cb6be291be3aaf123756 0a0ddd1fd4ea5cf502120f	epoch 174
Aug. 28, 2025	45hzuq7TBR3J89EXkAmZuqY9Dgpcd6xFSq4U2DMY5b o2RUSJ4V7Y3QWpMAWGF7CQ8955U6XR2F4PUVbJhU5D nzs3c16dM9Dy	9267d1762b0f3262029be73e30f5158159c2f38e86 b9d745231e57141afccd0a	epoch 175
Sep. 3, 2025	49heVqhSzn9eoaatkooNjLHhSRV6XiitDeW4J92cgn ey8BFfuacZGmzSA3fRKEHooC7X9xzCP9VXN6uK7Xrp oXF35FXfQCP	d761a707408f9693f9a453501dc04df6c92b82309a 90f23884564dabfed70106	epoch 176
Sep. 10, 2025	42Vt47oLYrT7C1Ch3BbapKFZgs5Hip5m3RrRVT2dbj DT8NWs76gc77NgfZvzXpZnPYGgVZFf79T5TSKWSjFx Ywk4A77WGa6	91c313b9cb0cc45e03e2f6f97e9d61566f8d0636b4 bb3bf59c59022972caad09	epoch 177
Sep. 17, 2025	47GwPhLcnWshcbekVshrzxJzWXXfDRUrjb7T6CfR1H aaiokeBxwAsQnFp779bF6rW43giviWwYbsoT1KehsG nPL5L7v1vuF6	c9f5d5027465f4ff51538210e4fa110756e956c064 897f969c4a60863e227f0c	epoch 178
Sep. 24, 2025	44UsmtpAE5GC8U8vnLp7FqUfAYkWL5YYZJLNFdQrb4 6ePpSH58ydJ2QtfmEgr834AQphJYwsLvnJrE1uFh T38bQnTebXm	a5e32d32ea8d1aac9ed47b7679ecf2cc4884dc5b38 8d9b539fede7ae5389f603	epoch 179
Oct. 1, 2025	48Psv1UrxcrQY6m1ZaDMXSMt38kEvZNhjWNgiSmJoU L7BFjm5A4XkiBkt2ApF5ydqsDtaMfZK8WBT7PtavvK GMfZUdZqjUe	5b78ba1a936efe94acb8e13fce72ee3581267ef668 a9c0f8967883ab12394602	epoch 180
Oct. 8, 2025	48Psv1UrxcrQY6m1ZaDMXSMt38kEvZNhjWN5qTB5D9 6DN4K1EbbRM8WBTF0W3JP4AW288WTDp7VhStLu3D8F N3V2blw9z1H	1fbd6085b25183aadd0c241e94adb4379bfb145cd5 1b968c7bf068d171275902	epoch 181
Oct. 15, 2025	48BZD46hnnvGJmh5kn4py9oEupM8uL3ZobK59GDMWkZ BdHyB2ALiSD6rGa2u9inZgmTegfKciaanDYndFEw8o GHKmAcYEQTto	938e19ee3f4e0fc025e1f2b5d2eafb9bb7db899cce 00e2367d395e935a470209	epoch 182
Oct. 15, 2025	42y5h2kPKhKTW82xqf7XHMFUz32Hs8ubgCowd8Q4y5 RY8XqvnCEfzX2cCexyfsLtdD1BjT5mRMDHiBrC1t8C aT1RDeDsMrg	173ad08b17faf1a672ee8314c79e4d2e931ed85210 c925d722cb400a2c7c3405	epoch 182
Oct. 23, 2025	45w3hfgjzJjHiDSSVKx4nKdHawTGrWzr4WPT5LL4qe Nx4fyyRQ73cNiLGGrrJ5pDjP8LHeDJfTMCs1UN7eBp WTPy1YX7YCV	726d15c6d9963e41965d87e311f1e51ff5722badfa 824336e893fb01a11acb00	epoch 183
Oct. 19, 2025	48CzXZx9YkcTTKAP8qc2cMfFiXpLQpxDDVEDNn5mTr F5aX9thAY7eqfUzJkwqkXtaZhb7Ggv9rjCJYeYRzZf HKPjF2BbDtx	7b8f7098b3892b7d9fb9b9ab3f96559dde693e052a c60d034e5b4115f548e119	epoch 184
Nov. 6, 2025	4A6mfADoDhNEAodQChmXRTSgsK4gheMna73TebmsKw 4rRggore7U1p8No32pJytUPtfoS5xk11aDh93BzggZ phbkUykELdm	d696c09c6a95b91fbf709711f027797c9bcee4a3d7 3d86e0361e95126655fe0e	epoch 185

On  $t \in \mathcal{S}$ , we have  $\eta(t) = \eta(\alpha(t), \gamma)$  and  $q(t) = \rho(\alpha(t), \gamma)$ , hence

$$\mathbb{E}[\eta(t)q(t) \mid t \in \mathcal{S}] = \mathbb{E}[\eta(\alpha(t), \gamma)\rho(\alpha(t), \gamma) \mid t \in \mathcal{S}] = r_S. \quad (16)$$

Therefore,

$$\mathbb{E}[\eta(t)q(t)] = (1-p)a_H + pr_S. \quad (17)$$

Similarly, the denominator satisfies

$$\mathbb{E}[\eta(t)] = (1-p) \cdot 1 + p \mathbb{E}[\eta(\alpha(t), \gamma) \mid t \in \mathcal{S}] = (1-p) + p r_S. \quad (18)$$

Thus,

$$\bar{R}_{\text{switch}} \approx \frac{(1-p)a_H + pr_S}{(1-p) + p r_S}. \quad (19)$$

Always-honest revenue is

$$\bar{R}_{\text{honest}} = \mathbb{E}[\alpha(t)] = (1-p)a_H + pa_S. \quad (20)$$

We now compare (19) and (20). The inequality  $\bar{R}_{\text{switch}} > \bar{R}_{\text{honest}}$  is equivalent (since  $(1-p) + p r_S > 0$ ) to

$$(1-p) + p r_S > ((1-p)a_H + pa_S) \frac{(1-p)a_H + pr_S}{(1-p) + p r_S}. \quad (21)$$

TABLE III: Qubic's observed revenue overview

Period	Estimated $\alpha$	Observed Revenue	Main Chain	Qubic Total	Qubic Main
P1	0.3415	0.3386	508	208	193
P2	0.3213	0.3178	440	151	143
P3	0.3312	0.3476	421	157	146
P4	0.3349	0.3314	507	215	169
P5	0.3164	0.2778	605	243	175
P6	0.3223	0.2926	769	313	237
P7	0.3102	0.2939	611	237	194
P8	0.2578	0.2248	7429	2303	1693
P9	0.3436	0.3533	617	268	212
P10	0.2346	0.1793	1053	294	199
<b>Avg (P1-P10)</b>	<b>0.2802</b>	<b>0.2529</b>	<b>12960</b>	<b>4389</b>	<b>3361</b>
<b>Global Average</b>	<b>0.2209</b>	<b>0.2114</b>	<b>55937</b>	<b>13000</b>	<b>11871</b>

Expanding the right-hand side and rearranging terms yields the equivalent condition

$$r_S > \mathbb{E}[\alpha(t)] e_S + (1 - p)(a_S - a_H), \quad (22)$$

which is exactly (9). The final sentence follows because (9) does not require  $\mathbb{E}[\alpha(t)] > \alpha_{\text{th}}$ ; it only requires that the efficiency-weighted selfish gain within  $S$  dominates the efficiency penalty and the selection effect captured by  $(1 - p)(a_S - a_H)$ .